Int J Adv Manuf Technol (2017) 93:89–102
DOI 10.1007/s00170-015-7773-z

ORIGINAL ARTICLE

Investigations on mechanical and structural aspects of ultrasonic hybrid polymer mixture welding for industrial applications

S. Arungalai Vendan[1] · **T. Chinnadurai**[1] · **K. Senthil Kumar**[2] · **N. Prakash**[3]

Received: 22 April 2015 / Accepted: 28 August 2015 / Published online: 22 September 2015

Abstract Polycarbonate (PC) and ABS materials have several beneficial characteristics which facilitates its application in various industrial sectors, while developing products based on these polymers it is essential to enable the scope of its weldability feature. Considering this critical factor, researchers have been involved in investigating the weldability behavior of the above-mentioned polymers. However, there are no complete reports addressing the feasibility of welding of polymer mixtures. It has been observed that combination of two polymers with proper understanding of inbuilt chemical structures has yielded a hybrid polymer whose properties in terms of its strength, chemical bonding, structural integrity, and range of flexibility are higher. Hence, in this study, a pivotal attempt is made to develop a hybrid polymer with a combination of 60 % PC and 40 % ABS. Further, the polymer is subjected to ultrasonics to examine the conduciveness of this material for welding. The parameters controlling the weldability using ultrasonic's are also varied within a range in order to identify the optimum parametric values. Subsequently, the welded specimens are tested for evaluating its strength and quality. Tests from the insight of chemical engineering is also carried out to access the chemical structural stability and to monitor the formation of the plastic which preferably adopts a thermoplastic feature. The results establish the feasibility and credibility of these polymers for welding which is the industrial demand.

Keywords ABS · PC · Ultrasonic welding · Polymers

✉ S. Arungalai Vendan
arungalaisv@yahoo.co.in

[1] Industrial Automation and Instrumentation Division, SELECT, VIT, Vellore, India

[2] Department of Electronics and Instrumentation, Veltech Technical University, Avadi, Chennai, India

[3] Department of Chemistry, Thangavelu Engineering College, Chennai, India

1 Introduction

Polymers have found enormous applications in domestic use, packaging, food and beverage, industrial purpose, and automotive industry. Advanced and hybrid plastics and polymer blends are playing an important role in vehicle interior, exterior, body, and structural components [1]. Extensive range of polymers has been devised and fabricated for the different applications with an assortment of additives and fillers. Polymers are intricate and giant molecules. Owing to the interlinking structures, there may arise several complexities. Thermoplastics linked or branched polymers are prone to melting upon application of heat. Polymers can be subjected to continuous molting and de-molding within a specified range. Thermoplastics are categorized further as amorphous, crystalline, and liquid crystalline. ABS, a copolymer, comprises polymerized styrene and acrylonitrile with polybutadiene and exhibits a balanced combination of mechanical toughness, good dimensional stability, chemical resistance, and electrical insulating properties. Considering the several positive features of ABS, its demand has been gargantuan. Apparently, it is imperative to ascertain the machinability and weld ability of this material to cater to the structural requirements. In case of welding, both the materials must have chemical compatibility and the difference between the melting temperatures of those materials should not be very high [2].

Polycarbonate (PC) is a multifunctional and high-performance amorphous thermoplastic, as it offers unique salient features such as high impact strength, transparency, heat

resistance, dimensional stability, and excellent electrical properties. PC also exhibits excellent, color ability, high gloss, sterilizability, flame retardancy, biocompatibility, high heat distortion temperature (HDT), and strain resistance. The other prominent aspect of PC is its non-specific melting point, as exhibited by typical crystalline polymers, but has a high glass transition temperature of approximately 150 °C. Besides, it is rather difficult to process PC, owing to its high melt viscosity that hinders the fluidity and the residual stress resulting from the process causing fractures [3]. PC-ABS blend tends to enhance the flowability, processability, electro-plating, performance machinability, and appearance.

Ultrasonic welding appears to be a suitable method in which high-frequency ultrasonic vibrations are used for melting and joining materials. The parts to be welded are held together under pressure and are subjected to ultrasonic vibrations, which have low amplitude (1–25 μm), usually at a frequency of 20 kHz. The alternating stresses induced generate heat at the parts being joined, specifically focused at the interface of the weld, where heat is generated by intermolecular friction and repeated forced contact. The mechanical properties of the materials to be welded, shape of the components, joint surface treatment, and process parameters, significantly govern the ultrasonic welding of specimens. The efficiency of energy transmission is related to the distance between the horn and the surface to be welded. When this distance increases, the efficiency decreases. Therefore, the weld necessitates higher amplitude of vibration, longer weld time, and higher air pressure to achieve good weld quality.

Heat equations governing the ultrasonic joining process are provided in Eq. 1.

$$Q_{\text{avg}} = \omega\varepsilon\,{}_0^2E^{''}/2 \tag{1}$$

The average heating rate (Q_{avg}) is dependent on the loss modulus of the material (E''), the frequency (ω), and the applied strain (ε_0):

$$C_{\text{p}}(t)\rho(t)\frac{\partial T}{\partial x} = \frac{\partial}{\partial x}\left[C(t)\frac{\partial T}{\partial x}\right] + Q(x,t) \tag{2}$$

where $C_{\text{p}}(t)$ is the specific heat (J g^{-1} K), $\rho(t)$ is the density of the material (g m^{-3}), $C(t)$ is the thermal conductivity (W m^{-1} K), and Q (x,t) is the heat generation function (W m^{-1} K) as in Eq. 2.

Loss modulus of thermoplastics is dependent on temperature. As the melt or glass transition temperature is approached, the loss modulus increases and higher mechanical energy is converted into thermal energy. Temperature at the weld interface rises instantaneously after heating is initiated, at a rate of around 1000 °C s^{-1}. As the vibration inside the parts continues, the energy directors become hotter since the heat generated is higher than the losses due to conduction and convection. Once the temperature at the weld interface exceeds the melting temperature, the thermoplastic material starts to flow on application of pressure; the flow of the molten polymer can be described as the squeeze flow between two plates.

The degree of adhesion relies on the degree of real contact at the molecular level which clearly emphasizes on the fact that diffusion is a critical phenomenon in accomplishing good weld strength. In ultrasonic welding, contact pressure, which affects the time-dependent interfacial contact area, will influence the diffusion. Thus, it is necessary that sufficient time is allowed for contact area creation to result in efficient diffusion. The relationship between weld strength and the creation of contact area through which diffusion can occur over time is described by the following equation:

$$\sigma_{Ad}(t) = \int_0^t [A(T)/A_{\max}]\{[\delta N(t-T,x,y)/\delta T]E_{mol}\}^{1/2}dxdydt \tag{3}$$

where $A(T)$ is the time-dependent interfacial contact area, which is a function of the applied contact pressure (Eq. 3). When the contact pressure is applied, $A(T)$ can be assumed to be linearly proportional to the pressure. Otherwise, viscoelastic material properties need to be taken into account.

Tsujino et al. [4] observed an improvement in the joint characteristics of ultrasonic plastic welding by using higher-frequency vibrations owing to the larger vibration loss in the plastic material. The welding characteristics of a 1.0-mm-thick polypropylene sheet were measured in for higher resonant frequencies. It was recorded that the welded area by fundamental and two higher frequencies were about three to four times that of the case where only the fundamental frequency is driven. A model for wave propagation in viscoelastic materials to predict vibration amplitude at the joint interface was developed by Benetar and Cheng [5]. Accomplishment of a reasonable and acceptable ultrasonic plastic welding requires high displacement amplification of ultrasonic horns in order to melt the thermoplastics [6, 7]. They employed "vibrothermography," a technique that permits selective imaging of defects using thermal waves that is generated by ultrasound waves.

The mechanism involved is frictional heating or hysteresis that turns a dynamically loaded defect into a heat source identified by a thermography system. One major challenge of technology is the proper control of the temperature, pressure, and heating time in order to achieve a high-quality joint [8, 9];

Table 1 Ingredients percentage in polymer blends

Ingredients	Quantity of the ingredients (%)
Polycarbonate (PC)	60
Acrylonitrile butadiene styrene (ABS)	40

Table 2 Experimental trials with all input parameters

S. no.	Sample no.	Welding pressure (bar)	Welding time (ms)	Energy (W)	Amplitude (%)	Speed (m s^{-1})	Trigger pressure	Strength (N)
1	A	3	400	774	100	5	3	570.29
2	A	3.5	500	1479	100	5	3	791.68
	B	3.5	500	1702	100	5	3	803.84
	C	3.5	500	1742	100	5	3	819.33
	D	3.5	500	2035	100	5	3	826.58
	E	3.5	500	1600	100	5	3	798.97
3	A	4	500	1300	100	5	3	798.34
	B	4	500	1179	100	5	3	785.83
	C	4	550	1223	100	5	3	792.50
	D	4	550	1400	100	6	3	813.68
	E	4	550	2200	100	6	3	858.48
	F	4	550	1866	100	6	3	833.89
4	A	6	600	2141	100	6	3	916.82
	B	4.5	600	1660	100	6	3	811.84
	C	4.5	600	1642	100	6	3	807.99
	D	4.5	600	1547	100	6	3	797.26
5	A	5	650	1985	100	6	3	835.34
	B	5	650	1041	100	6	3	789.65
	C	5	650	1788	100	6	3	839.23
	D	5	650	2235	100	6	3	878.73
	E	5	650	2138	100	6	3	862.12
6	A	5.5	700	1475	100	6	3	827.76
	B	5.5	700	1164	100	6	3	815.90
7	A	6	750	1795	100	6	3	847.24
	B	6	750	1485	100	6	3	840.93
	C	6	750	1161	100	6	3	826.43

the morphology of a PC-ABS blend throughout the complete composition range needs an extensive investigation. The PC-rich blends showed dispersed ABS in a bead and string structure. With increasing ABS content, blend strength was more interconnected. To improve its mechanical properties, ABS needs to be blended with other high-performance engineering plastics, such as PC (Table 1) [10].

The PC-ABS blends are known to possess high impact strength and many other desirable properties. Furthermore, since it can be easily processed, PC-ABS blends have been widely utilized as an engineering thermoplastic [11].

PC-ABS alloy combines the good performances of PC and ABS. The heat resistance and tensile strength of ABS are improved, while in parallel, the melt viscosity of PC is reduced to improve the processing performance. Besides, there is a prominent relation of sensitivity of stress and impact strength of the thickness of products. The heat resistance, impact resistance, and rigidness of thin-walled products of PC-ABS blends are significantly improved compared with ABS.

Moreover, the possible features of the PC-ABS blend viz. glassy nature, high impact resistance and rigidness, improvement in service temperature −60~120 °C and HDT between 120 and 140 °C, better electrical properties, and flame retardance characteristics, are taken into attempt, and

Fig. 1 Injection molding machine model no. MPE-TLH-1-FAC- 60

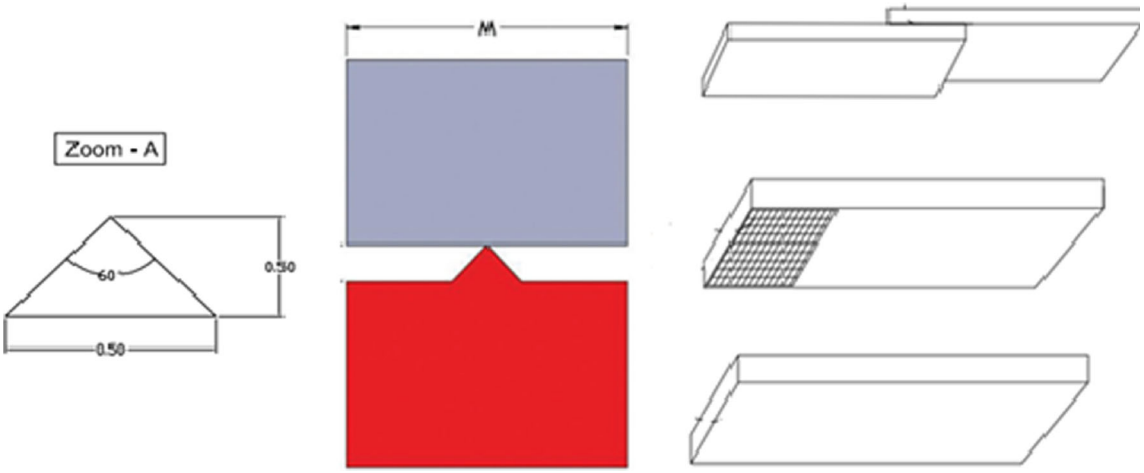

Fig. 2 Energy director design and samples

feasibility of welding using ultrasonic is thoroughly investigated. The literature survey provides a good insight into the fundamentals of the process and strength while the microlevel phenomenon and the possible causes have not been dealt in details. Further, the surface morphology is another critical area for experimental investigations which are limited in the available literature. Hence, in this study, an attempt is being made to address their interactive research concerns.

2 Experimentation

Considering the marked improvement of the heat resistance and tensile strength of ABS and reduced melt viscosity of PC, the preferred blend that appears to be feasible for multidimensional industrial applications is joined using ultrasonic welding. This investigation basically focused on lap joining of two specimens, one of them impinged with energy directors. This is followed by application of pressure by the horn of the ultrasonic welding equipment whose frequency power rating is 20 kHz and 2000 W, respectively.

Welding was performed for five sets of samples by varying process parameters whose details are tabulated in Table 2. This procedure is basically carried out to determine an approximate range in which the process parameters have to be maintained in order to accomplish a reasonable and good weld. The fourth set of samples as detailed in Table 2 achieves the desired weld characteristics. Subsequently, the characterization and testing sequences are performed exclusively on these specimens. Further, a comparative study is made between the raw blend and the welded specimens.

2.1 Sample preparation

PC-ABS grains are procured from Associated Chemicals and Instruments, Chennai. They are mixed in 60–40 % ratio as indicated Table 1 and are subjected to preheating followed by mould preparation using injection molding equipment used for this investigation as shown in Fig. 1 (specification of machine: max. pressure range 105 kg cm^{-2}, maximum applied force 5 t, max. mold thickness 250 mm, heater capacity 1.5 kW). Two sets of the mould specimens are prepared, one

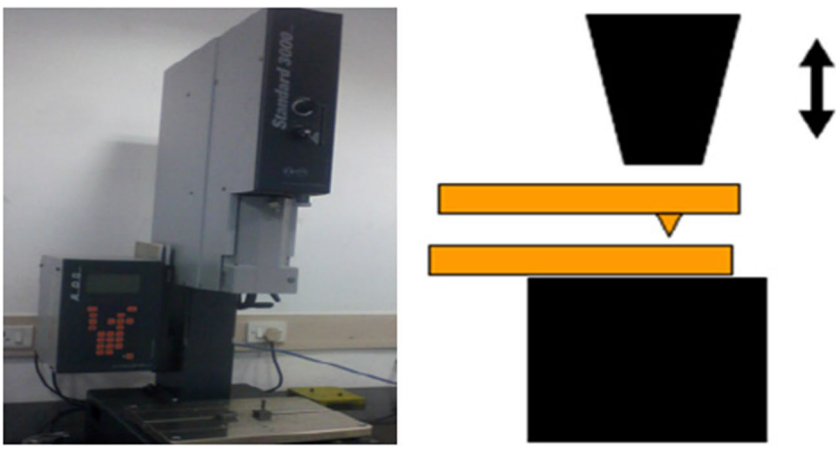

Fig. 3 Ultrasonic welding equipment and positioning of specimens in lap configuration

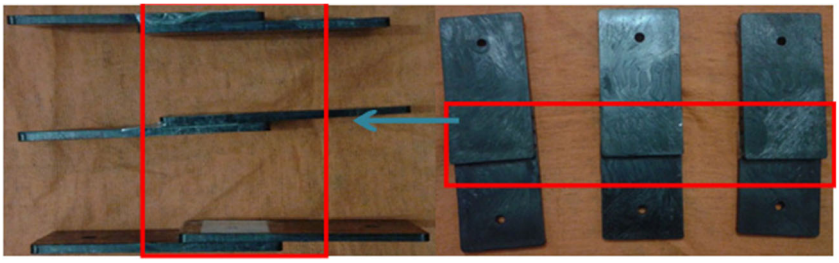

Fig. 4 Ultrasonically welded PC-ABS specimens

with energy director and other without energy director. Triangular energy director is used for this study whose angle of inclination and position are illustrated in Fig. 2.

a

Polycarbonates (PC)

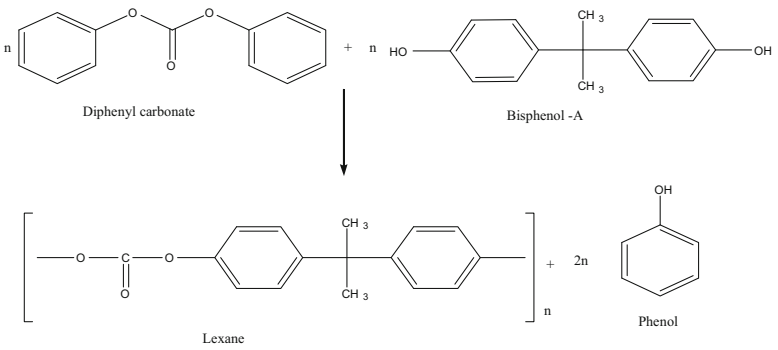

b

ABS Structure

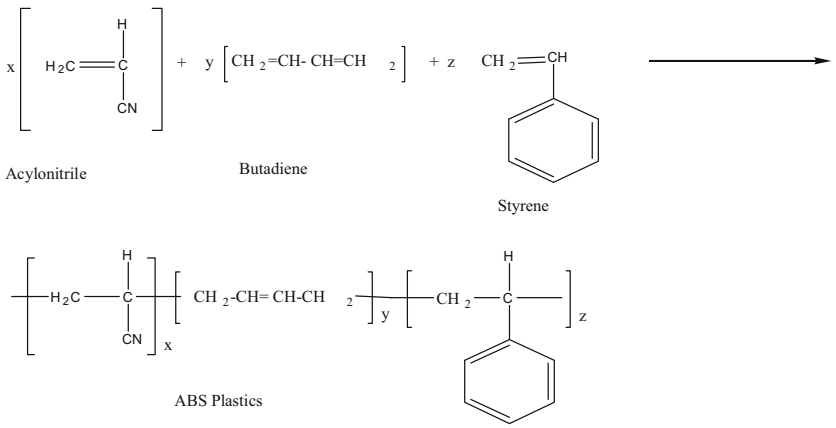

c

PC-ABS blend chemical components

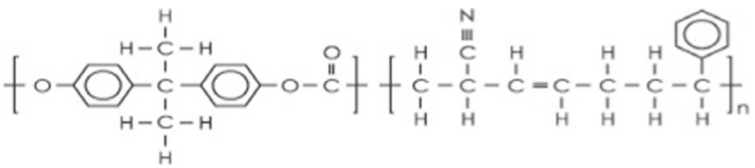

Fig. 5 **a** Polycarbonate chemical structure. **b** ABS plastic chemical structure. **c** PC-ABS blend chemical components

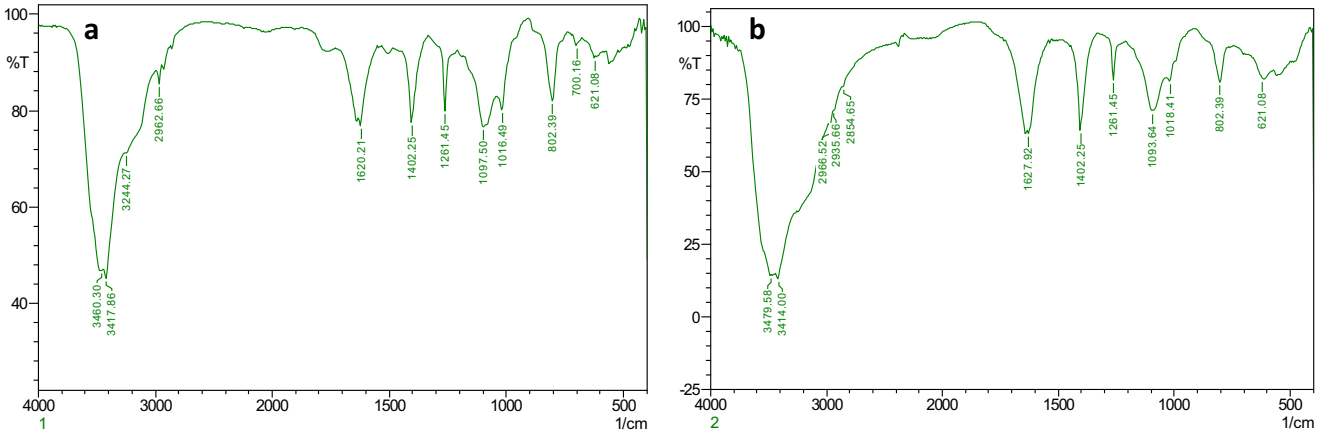

Fig. 6 FTIR analysis results **a** for the non-welded specimen and **b** for the welded specimen of first samples

Figure 3 shows the equipment and positioning of specimens in lap configuration. There are four phases of ultrasonic welding. During welding, horn vibration is perpendicular to the joint surface, and the point of the energy director, if there is one, is forced into contact. The energy director melts and flows onto the interface during this phase, and the heat generation is higher. The second phase corresponds to the meeting of part surfaces while the melting rate increases. In phase 3, steady-state melting occurs and a melt layer forms at the interface.

The maximum displacement is reached in phase 4, and an additional melt is squeezed out of the joint interface in the form of spruce. Intermolecular diffusion during melt flow results in new polymer chain entanglements between the two parts being welded, serving to produce high weld strength. After a set weld time and/or power level and/or distance has been reached, the welder is turned off, but the horn pressure is maintained as the weld cools [12].

3 Results and discussion

Figure 4 shows the welded region when PC and ABS have been blended and joined together in the lap configuration. From the visual inspection, it is clearly evident that the bonding is good and there is no crack, voids are excessive materials flow squeezing out of the joint. The corresponding changes in the chemical structure of PC-ABS blend with application of pressure and heat are illustrated in Fig. 5a–c).

3.1 FTIR analysis

In Fig. 6a, b Fourier transform infrared spectroscopy (FTIR) spectrum of PC and ABS shows that broad band in the region 3437–3244 cm^{-1} is due to characteristic –OH stretching. The peak at 2962 cm^{-1} is attributed to C–H stretching vibrations.

Another strong and sharp peak at 1620 cm^{-1} may be due to O–H bending and peak at 1402 cm^{-1} is sharp attributed to C–H bending. The FTIR spectra relative to PC and ABS show absorption peak at about 3413 cm^{-1} of the hydroxyl groups and at 1037 and 1402 cm^{-1} related to C–O bonds. In the spectra of the blend film, we see interactions involving natural and synthetic polymers: C═O at 1620 cm^{-1}. That is, the peak at 902 cm^{-1} may be due to Si–O stretching, and the peak from the FT-IR data concluded that polymer composite thoroughly mixed with carbon, −OH stretching, and Si–O.

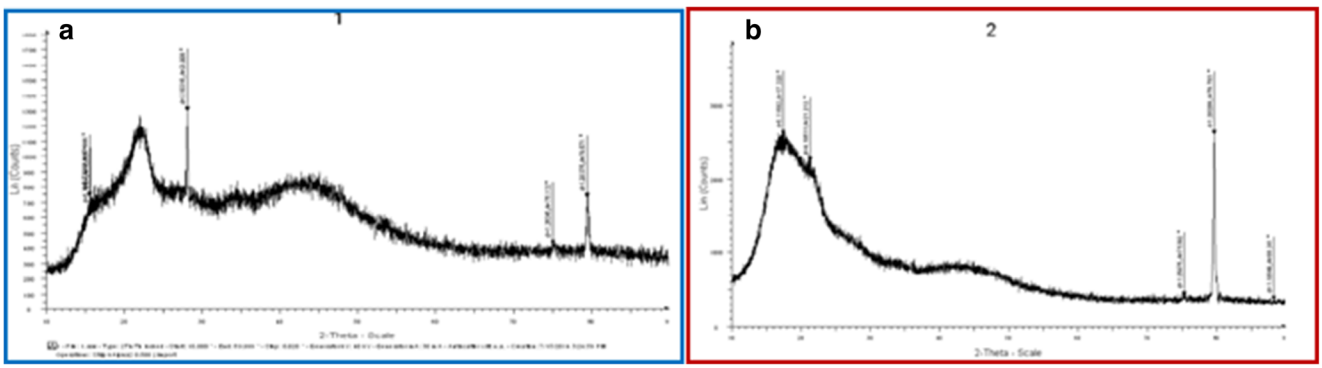

Fig. 7 XRD results **a** for non-welded specimen and **b** for welded specimens

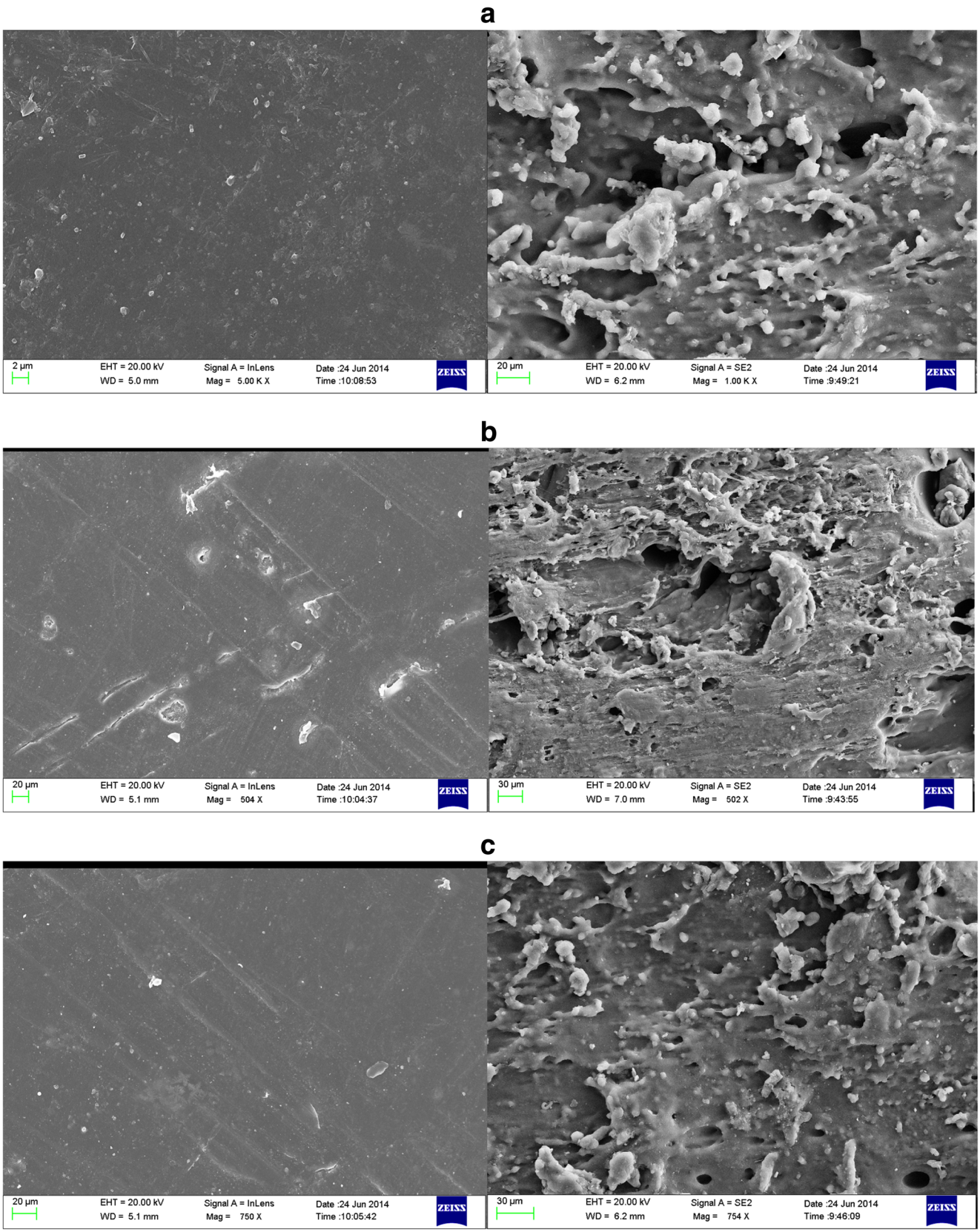

Fig. 8 **a**–**e** SEM images of all samples showing the non-welding and welding region images

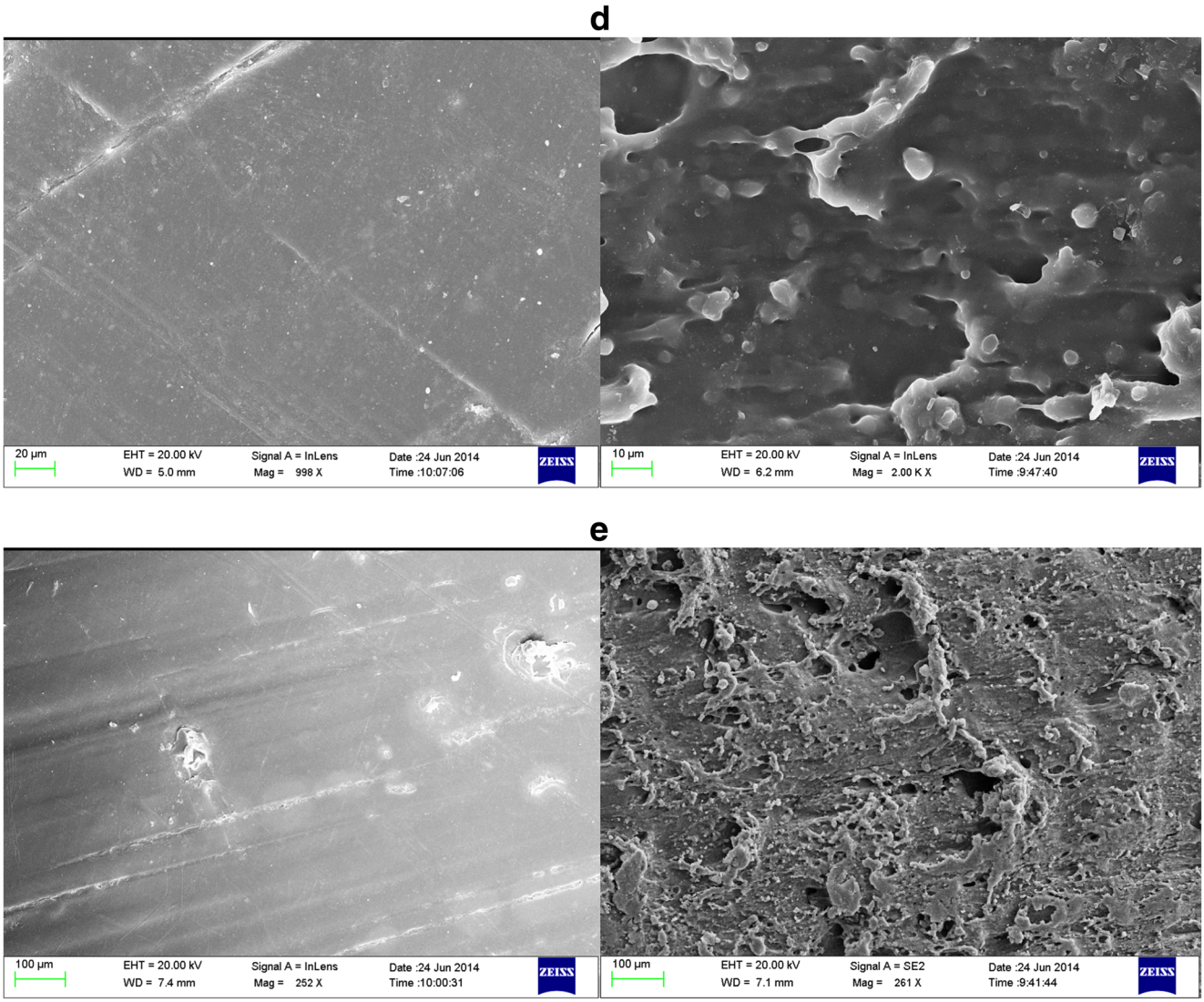

Fig. 8 continued.

3.2 XRD analysis

Polymers exhibit varying amounts of crystalline and hence can be characterized by X-ray diffraction technique.

X-ray diffraction (XRD) techniques are used to identify the state of polymer, i.e., either crystalline, semicrystalline, or amorphous etc., to calculate percentage of crystalline nature, and to identify polymers and fillers and their quantification. Plastic deformation of crystalline phase usually causes the accumulation of defects and the generation of chemical disorder which consequently results in the deformation-induced crystal-to-amorphous transition. Figure 7a, b shows XRD patterns of PC and ABS polymer composites. PC exhibits reflection fall at about 2 theta. The PC-ABS blend shows two diffraction peaks at 18° and 41°, which are the characteristics of crystalline peaks of ABS and hydrated crystalline structure of PC, respectively. PC-ABS blend the intensity of diffraction peak at 18° for ABS becomes flat and broad gradually.

The peak of the hydrated crystalline structure of PC at 41° shows the same tendency. Thus, it becomes evident the crystalline nature of ABS and PC. This phenomenon is due to the significant hydrogen bonding interaction among PC and ABS molecules. In other words, there is an improvement in the compatibility between PC and ABS. PC-ABS indicates the peak at 2 theta which becomes flat and broad gradually to higher diffraction value of 41° is proved by the chemical interactions. The average crystallinity index (ratio of the areas) of pure ABS was reduced. So, the chemical structure inhibits close packing of the polymer chains by reducing the degree of freedom in the 3-D conformation, preventing the formation of crystalline regions. This reduction of crystallinity would play a crucial role on influencing the blend degradability, water absorption, and swelling.

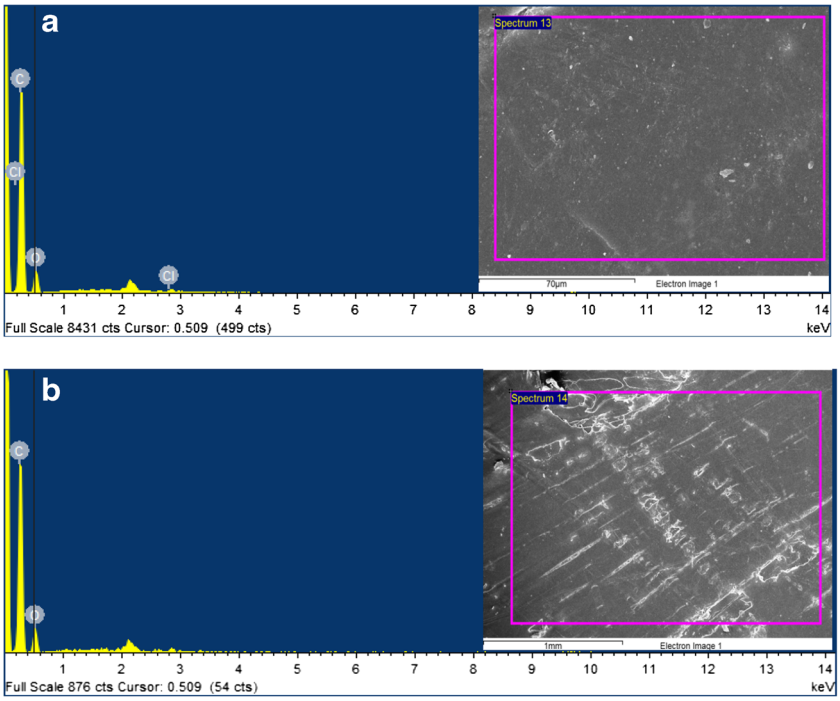

Fig. 9 **a**, **b** EDAX showing the non-welding region chemical components

3.3 SEM-EDAX analysis

Investigating the deformed polymer morphology is essential in understanding the form and structure at welded polymer interface. The deformed ridges are the prominent features of the welded samples. The number and the depth of deformed ridges are related to the welding time, temperature, and weld pressure content. At short welding times, the depth of interpenetration across interface is considerably small and the strength and energy are low at the welded interface. Figure 8 shows SEM micrographs of samples with different blend ratios of PC-ABS.

The white particles in Fig. 8 are the peaks. The higher peaks describe the good melting conditions of energy

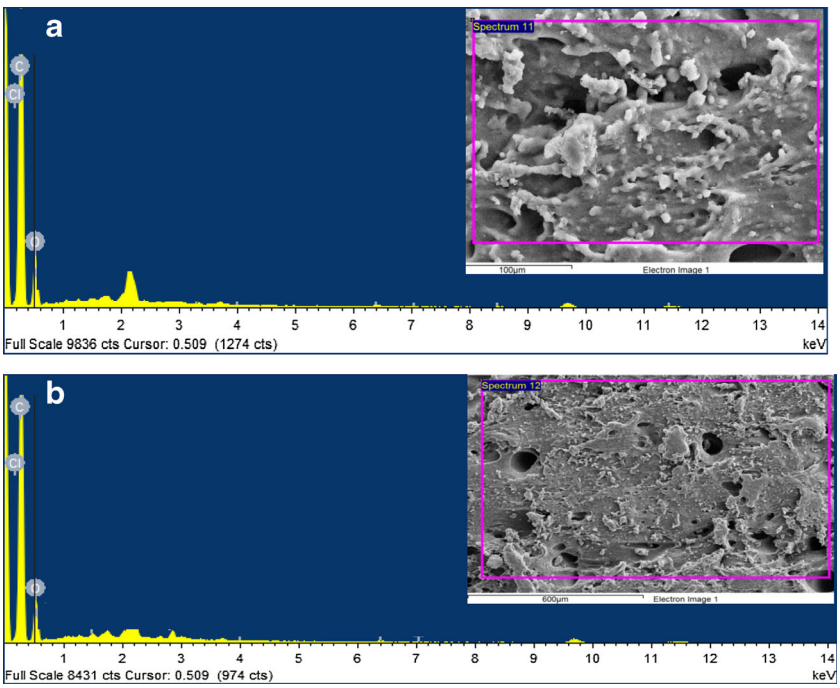

Fig. 10 EDAX and SEM for welded region of the specimen

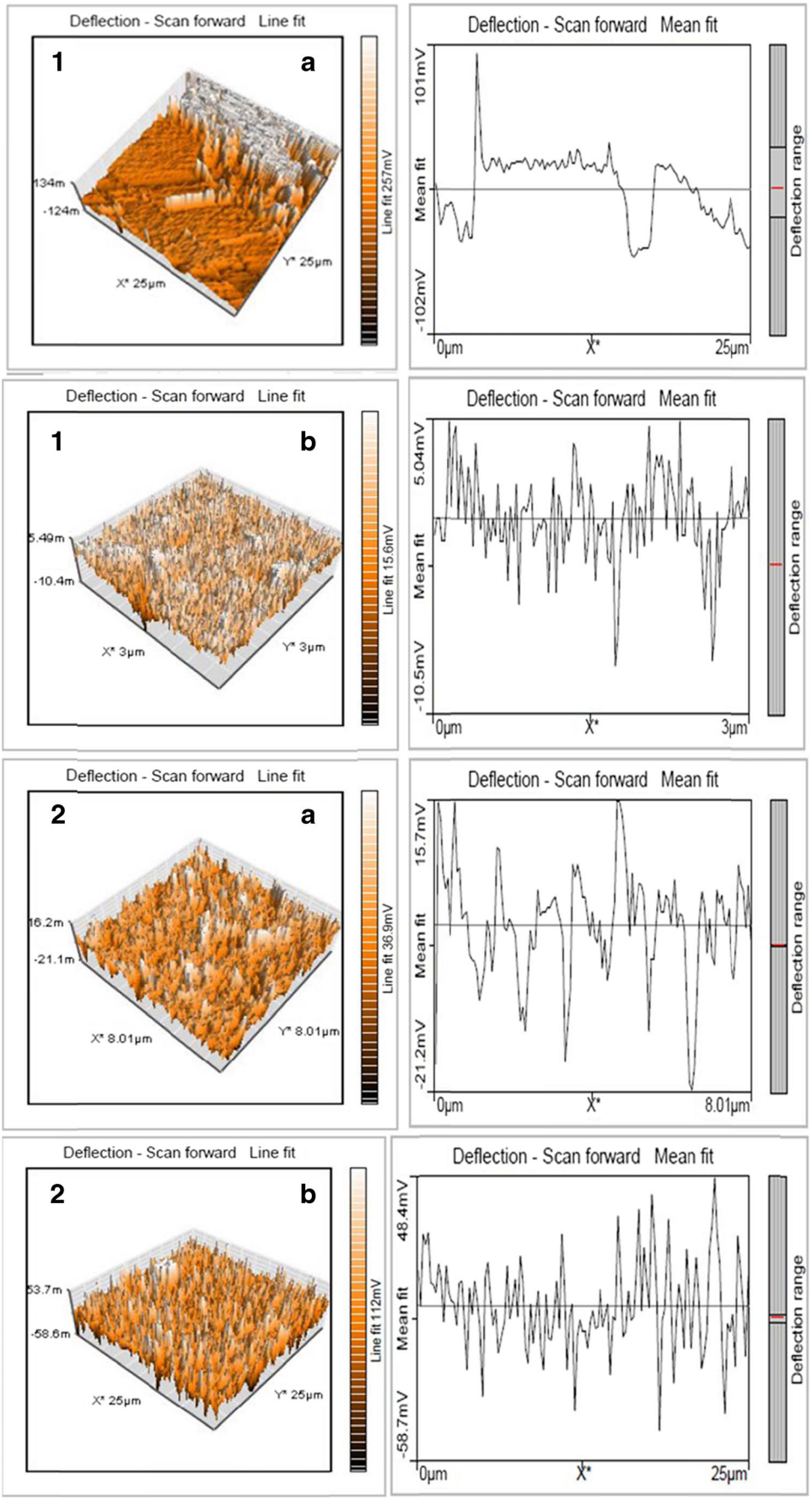

Fig. 11 AFM images with corresponding graph

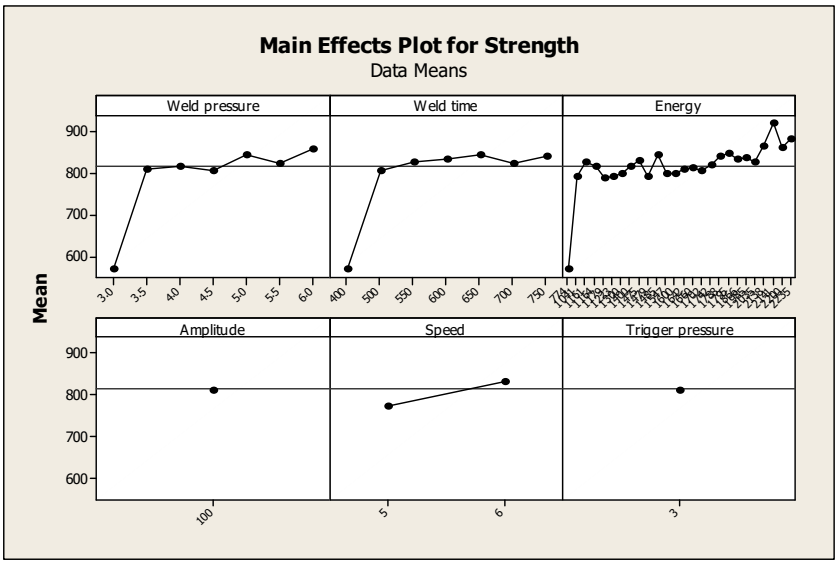

Fig. 12 Main effect plot for strength vs weld pressure, weld time, energy, amplitude, speed, and trigger pressure

directors, which are well dispersed in both PC and ABS phases. The component with the higher content is the continuous phase, and the minor component is dispersed particles. The ABS-rich blends had conventional blend morphology with PC domains dispersed in ABS.

Energy-dispersive X-ray spectroscopy or elemental-dispersive analysis by X-rays (EDAX) is used for the quantitative analysis. In this procedure, while a beam of electron strikes a specimen, a fraction of the incident electrons excites the atoms of the specimen, which tends to emit X-rays while returning to their ground state. The energy of these X-rays is strictly related to the atomic number of the elements excited, and henceforth, their detection forms the basis of elemental analysis in the electron microscope [13]. EDAX results shown in the Figs. 9 and 10, along with the SEM, have been obtained for welded and non-welded region. This analysis is performed to observe the changes occurring in the materials due to the pressure and heat applied. It can be clearly noticed that there is absence of any impurities or intricate compounds which may weaken the weldments. The diffusion of the molecules appears to be uniform in the welded region on the amorphous nature improves the integrity of the weldments. There is OH stretching phenomenon that is natural which again aides in better bonding.

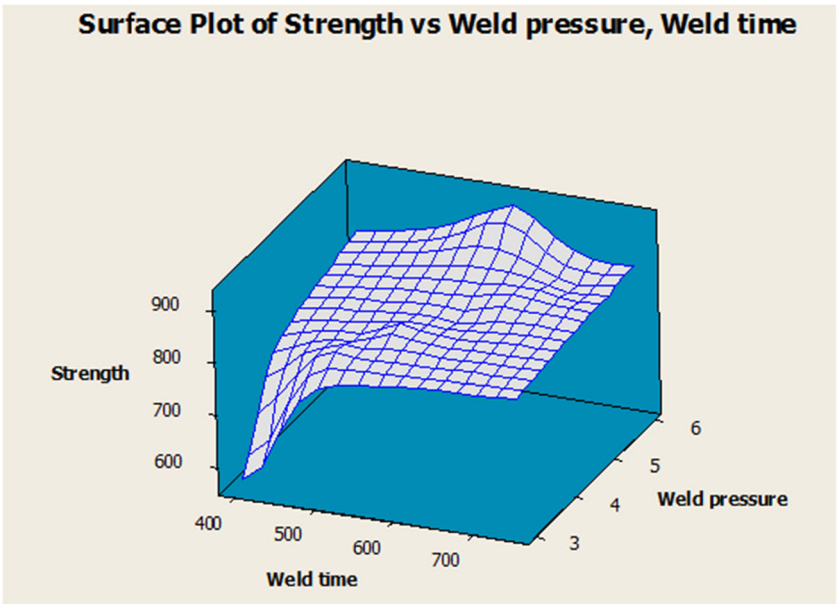

Fig. 13 Strength vs weld time vs weld pressure

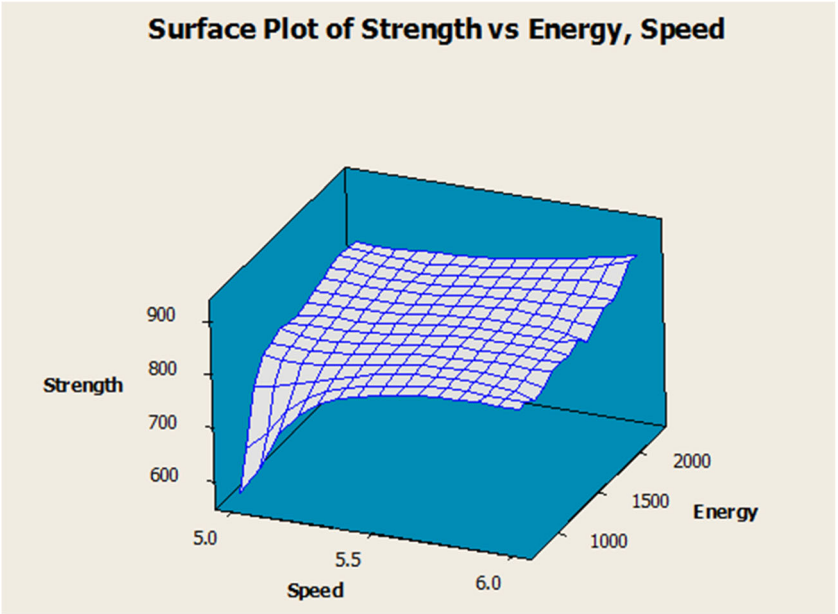

Fig. 14 Strength vs energy vs speed

3.4 AFM analysis

The amplitude parameters of a sample are described by parameters which give information about statistical average values, shape of the histogram heights, and other extreme properties. The average roughness (Ra) is the mean height as calculated over the entire measured length/area. Maximum peak to valley height roughness (Rt) is the vertical distance between the highest and lowest points in the evaluated length/area and describes the overall roughness of the surface. Root-mean-square (RMS) roughness (Rq) is the square root of the distribution of surface height and is considered to be more sensitive than the average roughness for large deviations from the mean line/plane and is also used in computing the skew and kurtosis parameters. Ten-point mean height roughness (Rz) is the difference in height between the average of five highest peaks and five lowest valleys in the evaluation profile/surface and is more sensitive to occasional high peaks or deep valleys than Ra. Roughness skewness (Rsk) is used to measure the symmetry of the variations of a profile/surface about the mean line/plane and is more sensitive to occasional deep valleys or high peaks [14]. Usually, Rsk is used to distinguish two profiles of the same Ra or Rq values but of different shapes. Roughness kurtosis (Rku) is used to measure the distribution of the spikes above and below the mean line/plane [15]. Figure 11 shows the three-dimensional atomic force microscopy (AFM) micrographs of the surface of PC-ABS. The micrographs reveal that the films do not show continuous long

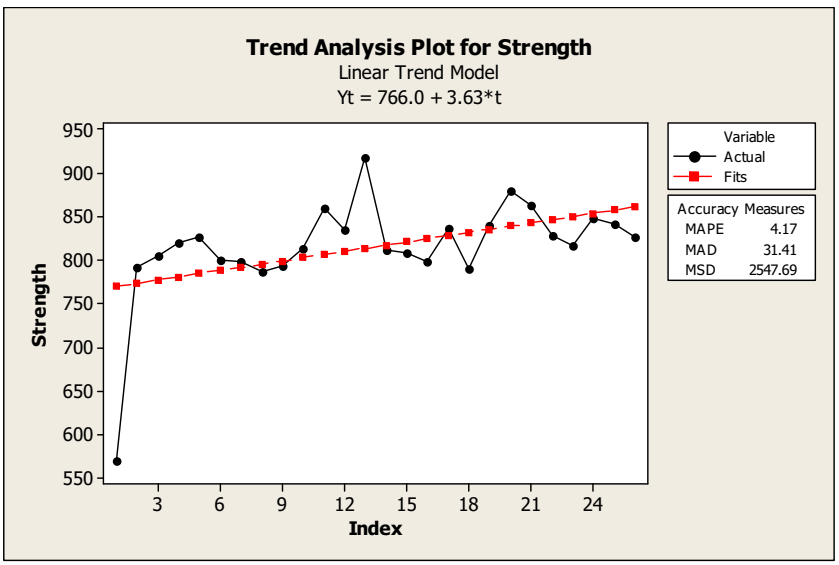

Fig. 15 Trend analysis for strength actual line and fit line

trenches or blotches, which are indicative of a crack-free and pinhole-free surface. The variations of the RMS roughness (Rq) of the Fig. 11 (1A, 1B, 2A, and 2B) films as a function of the film thickness are shown in Fig. 11 (1B, 2B). The RMS roughness increases with film thickness almost linearly. The increase in Rq content films is due to the size difference between PC-ABS weld time 300 ms and pressure was 3 bar, roughness is obtained at low value. Figure 11 (1A) shows the non-weld region (r=0.134 μm), and Fig. 11 (1B) shows a weld region roughness obtained at 0.137 μm. PC-ABS sample with high weld strength of 916.86 N obtained from weld time is 600 m and weld pressure was 6 bar, for this values roughness obtained values from showed Fig. 11 (2A) non-weld strength 22.7 μm and Fig. 11 (2B) shows the welded region of same process parameters obtaining roughness is 23.8 μm.

4 Process parameter analysis

Figure 12 shows the process parameters controlling the welding quality and strength are the weld pressure, weld time, energy, amplitude, speed, trigger pressure, etc. Based on the graphical analysis, weld pressure, weld time, energy, and speed play a significant role in the weld strength. Surface plot graph shows the weld pressure, weld time contribution of the strength, time and pressure increases strength to certain level, thereafter weld strength has been reduced owing to the high pressure squeeze of melted materials.

Figure 13 shows the dependency pattern between the strength vs weld time and weld pressure. When the pressure is high at 6 bar and the time is 600 ms, the value of weld strength achieved is of maximum. When the weld squeezes, time reaches maximum, pressure also reaches maximum, and the weld strength is considerably reduced, because of high weld time which is around 700 ms wherein the energy director melt index is high, which squeezes the melted materials out of the weld parts leading to reduction in the weld strength.

Figure 14 shows the plot for strength vs speed and energy. It may be observed that as the speed increases, strength also increases while ensuring that the energy is maintained at low level. Subsequently, if the energy increases, strength slightly increases. However, the increases in strength are low. Figure 15 shows the trend analysis of actual vs fit line. Based on this graph, maximum actual points are fitted with fit line. The maximum strengths for various peak levels are obtained when the weld pressure and weld time were maximum.

5 Conclusions

This research study concentrates on determining the feasibility of ultrasonic welding for a polymer blend comprising PC and ABS. Material fabrication has been done with energy directors embedded on it. The specimens are further subjected to pressure and vibrations by means of ultrasonic process. Maximum heat transfer along with uniform distribution is ensured by using triangular energy directors. Examinations are conducted on the weld specimens to understand the various phenomenons occurring to explore the possible causes and to determine surface and structural aspects. Through this study, the following conclusions were drawn:

1. During the welding process, there is _OH and C_H stretching vibrations. Sharp peaks also attribute to the CH bending as observed from FTIR images.
2. The polymer blends are thoroughly mixed with carbon.
3. There is a significant hydrogen bonding interaction among PC and ABS molecules in the weldment. The crystallinity index has been reduced. Chemical structure exhibits close packing.
4. From the SEM images, it was noticed that there is higher content distribution in the continuous phase and minor content distribution in dispersed particles. The ABS-rich blends had a conventional morphology with PC domains dispersed in ABS.
5. The weld strength directly depends on the weld time and pressure up to a specified range. These inferences and conclusions establish the feasibility of ultrasonic welding process for joining thermoplastic polymer blends.

References

1. Russek UA, Poggel M, Otto G, Koeppe A (2003) Advances in laser beam welding of polymers and automotive prospects. Proceedings of the 9th International Conference: TPOs in Automotive, Maastricht, the Netherlands, 51–60
2. Baylis B et al (2002) Welding thermoplastic elastomers to polypropylene with a diode laser. Proceedings of the 21st ICALEO, Scottsdale, AZ, USA
3. Sohn J-I et al (2003) Effect of a reactive-type flame retardant on rheological and mechanical properties of PC/ABS blends. J Mater Sci 38:1485–1491
4. Tsujino J et al (2002) Ultrasonic plastic welding using fundamental and higher frequencies. Ultrasonics 40:375–378
5. Benatar A, Cheng Z (1989) Ultrasonic welding of thermoplastics in the far field. Polym Eng Sci 29(23):1699–1704
6. Kim SR et al (2011) Design of highly uniform spool and bar horns for ultrasonic bonding. IEEE Trans Ultrason Ferroelectr Freq Control 58:2194–2201
7. Saboktakin A et al (2010) Finite element analysis of heat generation in ultrasonic thermography, in: 10th International Conference on Quantitative Infrared Thermography, July, Quebec (Canada)
8. Ageorges C et al (2001) Advances in fusion bonding techniques for joining thermoplastic matrix composite: a review. Compos Appl Sci Manuf 32:839–857
9. Lee MP, Hiltner A (1992) Polymer 33(4):685–697
10. Suarez H, Barlow JW, Paul DR (1984) J Appl Polym Sci 29:3253

11. Maurar FHJ, Palmar JHM, Booij HC (1985) Rheol Acta 24:243
12. Handbook of plastic joining (a practical guide), Plastic design library. ISBN 1-884207-17-0
13. Nandre SJ et al (2012) Study of growth, EDAX, optical properties and surface morphology of zinc tartrate crystals. J Nano Electron Phys 4(4):04013. (4pp)
14. Ala'eddin AS, Ramli N, Poopalan P (2010) AFM study of multilayer sool-gel BaxSr1-xTiO3 thin films. Jordan J Phys 3(2):61-68
15. Gadelmawlaa ES, Kourab MM, Maksoudc TMA, Elewaa IM, Solimand HH (2002) J Mater Proc Tech 123:133